catalysts

MDPI

Article

Metal(II) Coordination Polymers from Tetracarboxylate Linkers: Synthesis, Structures, and Catalytic Cyanosilylation of Benzaldehydes

Yu Li [1,†], Chumin Liang [1,†], Xunzhong Zou [1], Jinzhong Gu [2], Marina V. Kirillova [3] and Alexander M. Kirillov [3,4,*]

1 Guangdong Research Center for Special Building Materials and Its Green Preparation Technology/Foshan Research Center for Special Functional Building Materials and Its Green Preparation Technology, Guangdong Industry Polytechnic, Guangzhou 510300, China; liyu@gdip.edu.cn (Y.L.); liangchumin@gdip.edu.cn (C.L.); zouxunzhong@gdip.edu.cn (X.Z.)
2 College of Chemistry and Chemical Engineering, Lanzhou University, Lanzhou 730000, China; gujzh@lzu.edu.cn
3 Centro de Química Estrutural and Departamento de Engenharia Química, Instituto Superior Técnico, Universidade de Lisboa, Av. Rovisco Pais, 1049-001 Lisbon, Portugal; kirillova@tecnico.ulisboa.pt
4 Research Institute of Chemistry, Peoples' Friendship University of Russia (RUDN University), 6 Miklukho-Maklaya st., 117198 Moscow, Russia
* Correspondence: kirillov@tecnico.ulisboa.pt; Tel.: +351-218-419-396
† These authors contributed equally to this work.

Abstract: Three 2D coordination polymers, $[Cu_2(\mu_4\text{-dpa})(bipy)_2(H_2O)]_n \cdot 6nH_2O$ (**1**), $[Mn_2(\mu_6\text{-dpa})(bipy)_2]_n$ (**2**), and $[Zn_2(\mu_4\text{-dpa})(bipy)_2(H_2O)_2]_n \cdot 2nH_2O$ (**3**), were prepared by a hydrothermal method using metal(II) chloride salts, 3-(2′,4′-dicarboxylphenoxy)phthalic acid (H_4dpa) as a linker, as well as 2,2′-bipyridine (bipy) as a crystallization mediator. Compounds **1**–**3** were obtained as crystalline solids and fully characterized. The structures of **1**–**3** were established by single-crystal X-ray diffraction, revealing 2D metal-organic networks of **sql**, **3,6L66**, and **hcb** topological types. Thermal stability and catalytic behavior of **1**–**3** were also studied. In particular, zinc(II) coordination polymer **3** functions as a highly active and recoverable heterogeneous catalyst in the mild cyanosilylation of benzaldehydes with trimethylsilyl cyanide to give cyanohydrin derivatives. The influence of various parameters was investigated, including a time of reaction, a loading of catalyst and its recycling, an effect of solvent type, and a substrate scope. As a result, up to 93% product yields were attained in a catalyst recoverable and reusable system when exploring 4-nitrobenzaldehyde as a model substrate. This study contributes to widening the types of multifunctional polycarboxylic acid linkers for the design of novel coordination polymers with notable applications in heterogeneous catalysis.

Keywords: hydrothermal synthesis; coordination polymers; crystal structures; metal-organic frameworks; carboxylate ligands; heterogeneous catalysis

check for updates

Citation: Li, Y.; Liang, C.; Zou, X.; Gu, J.; Kirillova, M.V.; Kirillov, A.M. Metal(II) Coordination Polymers from Tetracarboxylate Linkers: Synthesis, Structures, and Catalytic Cyanosilylation of Benzaldehydes. *Catalysts* **2021**, *11*, 204. https://doi.org/10.3390/catal11020204

Academic Editors: Jorge Bedia and Carolina Belver
Received: 26 December 2020
Accepted: 29 January 2021
Published: 3 February 2021

1. Introduction

Functional coordination polymers (CPs) and derived materials have been of a special focus in recent years owing to important structural characteristics of these compounds [1–3], intrinsic properties [4,5], and a broad diversity of applications [6–10] including in the field of catalysis [11–17]. The development of new catalytic systems incorporating coordination polymers with target structures and functionalities continues to be a challenging area, since the assembly of CPs can be affected by a diversity of factors. These include the nature of metal centers, organic linkers and supporting ligands, stoichiometry, and various reaction conditions [18–24].

Aromatic carboxylic acids with several COOH groups are the most common building blocks for constructing functional CPs [14,15,17,19]. Within a diversity of such carboxylic

acids, semi-flexible linkers are especially captivating due to unique geometrical arrangements and conformational flexibility, which may lead to crystallization of unexpected metal-organic architectures [21–23,25].

On the other hand, cyanosilylation of carbonyl substrates is an interesting reaction for C-C bond formation [26,27], which is used for the preparation of cyanohydrins—key precursors for some pharmaceutical and fine chemistry products [28,29]. The use of transition metal complexes or coordination polymers in cyanosilylation reactions is gaining relevance as these compounds can behave as low-cost, efficient, and recyclable catalysts [25,30,31].

Considering our research focus on the design of CPs and catalytic systems on their basis [14,15,25], the main goal of this study consisted in the preparation of new metal-organic architectures, followed by their characterization and catalytic application in cyanosilylation of benzaldehydes. Thus, we selected an unexplored ether-linked tetracarboxylic acid, 3-(2′,4′-dicarboxylphenoxy)phthalic acid (H_4dpa, Scheme 1), and tested it as a principal building block for generating copper(II), manganese(II), and zinc(II) CPs. The use of H_4dpa as a linker can be justified by a number of relevant features of this tetracarboxylic acid. These features include (i) up to 9 possible sites for coordination (eight O-carboxylate sites and an O-ether site); (ii) two aromatic rings that can provide certain spatial flexibility and conformational adaptation owing to their separation by O-ether group; (iii) the fact that this carboxylic acid possesses good stability under hydrothermal conditions and remains little-explored in the synthesis of CPs.

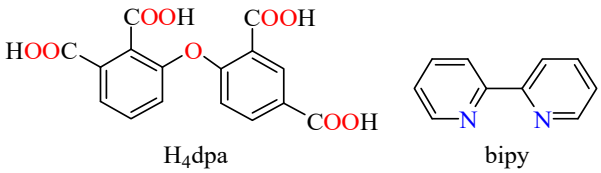

Scheme 1. Structural formulae of H_4dpa and bipy.

Thus, this work reports on the hydrothermal synthesis, characterization, thermal behavior, crystal structures, and catalytic application of 2D CPs derived from H_4dpa as a linker and bipy as a crystallization mediator. The obtained products $[Cu_2(\mu_4\text{-dpa})(bipy)_2(H_2O)]_n\cdot 6nH_2O$ (**1**), $[Mn_2(\mu_6\text{-dpa})(bipy)_2]_n$ (**2**), and $[Zn_2(\mu_4\text{-dpa})(bipy)_2(H_2O)_2]_n\cdot 2nH_2O$ (**3**) were also screened as potential catalysts for mild cyanosilylation of benzaldehydes into cyanohydrins. The influence of different reaction conditions and substrate scope was investigated, showing that the zinc(II) CP **3** is a particularly effective and recyclable heterogeneous catalyst.

2. Results and Discussion

2.1. Hydrothermal Synthesis

Aqueous medium mixtures composed of Cu(II), Mn(II), or Zn(II) chlorides with H_4dpa as a linker, NaOH as a base for deprotonation of carboxylic acid groups, and 2,2′-bipyridine as a mediator of crystallization were subjected to hydrothermal synthesis (3 days, 160 °C), resulting in the formation of three 2D coordination polymers as crystalline solids. These were formulated as $[Cu_2(\mu_4\text{-dpa})(bipy)_2(H_2O)]_n\cdot 6nH_2O$ (**1**), $[Mn_2(\mu_6\text{-dpa})(bipy)_2]_n$ (**2**), and $[Zn_2(\mu_4\text{-dpa})(bipy)_2(H_2O)_2]_n\cdot 2nH_2O$ (**3**) on the basis of standard solid-state characterization methods, namely infrared spectroscopy (IR), elemental analysis (EA), thermogravimetric analysis (TGA), powder (PXRD) and single-crystal X-ray diffraction. All compounds represent 2D metal-organic networks that are driven by ether-bridged tetracarboxylate nodes that show two distinct coordination modes, namely μ_4-dpa^{4-} in **1** and **3**, or μ_6-dpa^{4-} in **2** (Scheme 2).

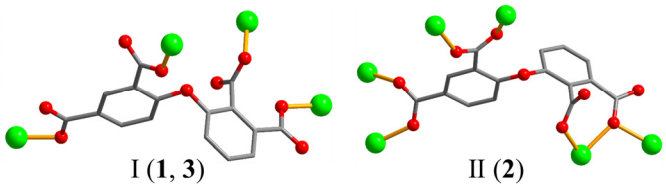

Scheme 2. Coordination modes of μ_4- or μ_6-dpa^{4-} linkers in **1**–**3**.

2.2. Structure of $[Cu_2(\mu_4\text{-dpa})(bipy)_2(H_2O)]_n \cdot 6H_2O$ (1)

The structure of a 2D CP **1** (Figure 1) comprises two Cu(II) centers (Cu1, Cu2), one μ_4-dpa^{4-} linker, two bipy moieties, and one terminal H_2O ligand per asymmetric unit. The Cu1 center is 4-coordinated and exhibits a distorted $\{CuN_2O_2\}$ seesaw geometry. It is formed by two carboxylate O atoms from a pair of μ_4-dpa^{4-} ligands and two bipy N atoms (Figure 1a). The Cu2 atom is five-coordinated and features a distorted $\{CuN_2O_3\}$ square-pyramidal geometry. It is constructed from two oxygen atoms from two μ_4-dpa^{4-} blocks, two bipy N atoms, and a terminal H_2O ligand.

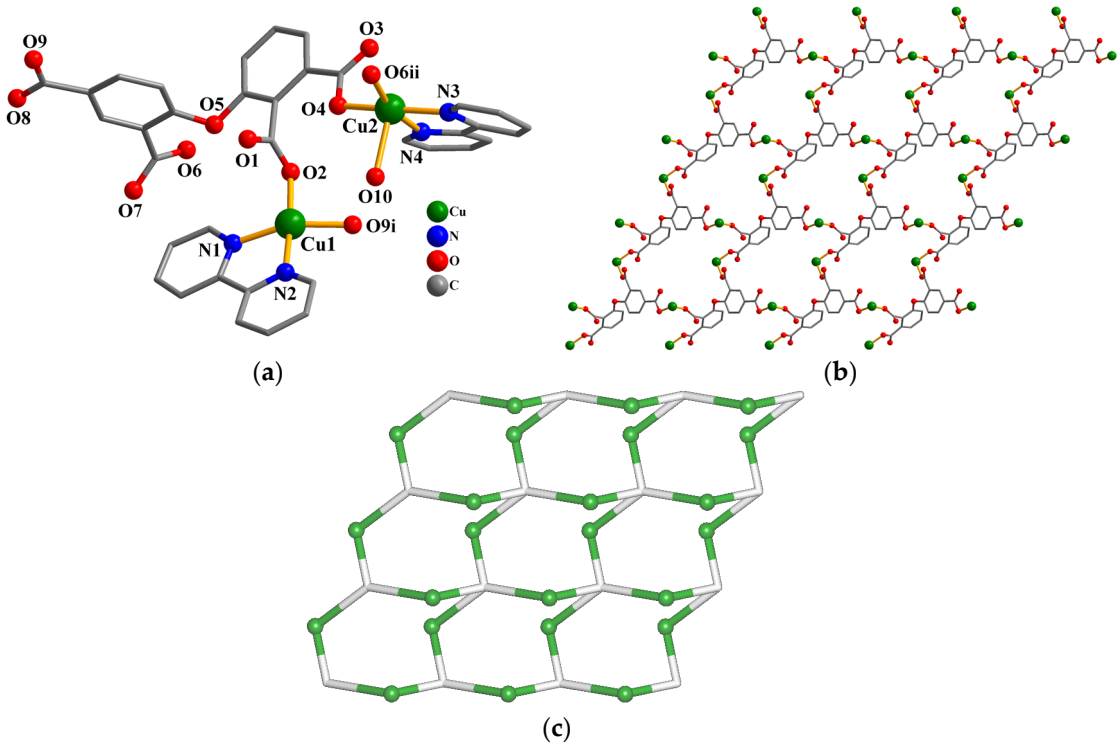

Figure 1. Structural fragments of **1**. (**a**) Coordination environment around Cu(II) atoms; H atoms are omitted for clarity. Symmetry codes: i = $x + 1, y, z + 1$; ii = $x + 1, y, z$. (**b**) 2D metal-organic layer; view along the *b* axis. (**c**) Topological view of 2D layer with a **sql** topology; view along the *b* axis; Cu centers (green balls), centroids of μ_4-dpa^{4-} nodes (gray).

The Cu–O [1.942(2)–2.345(3) Å] and Cu–N [1.992(3)–2.058(3) Å] bonds are typical for such a type of compounds [14,18,30]. The dpa^{4-} ligand behaves as a μ_4-linker with carboxylate moieties being monodentate (Scheme 2, mode I). In μ_4-dpa^{4-}, a dihedral angle between aromatic cycles and a C_{ar}–O_{ether}–C_{ar} angle are 86.34 and 115.93°, correspondingly. The μ_4-dpa^{4-} linkers connect four Cu atoms to assemble a 2D metal-organic layer (Figure 2b) which, after simplification, is described as a mononodal 4-linked net. It possesses a **sql** (Shubnikov tetragonal plane net) topology with a $(4^4.6^2)$ point symbol (Figure 1c) [32,33].

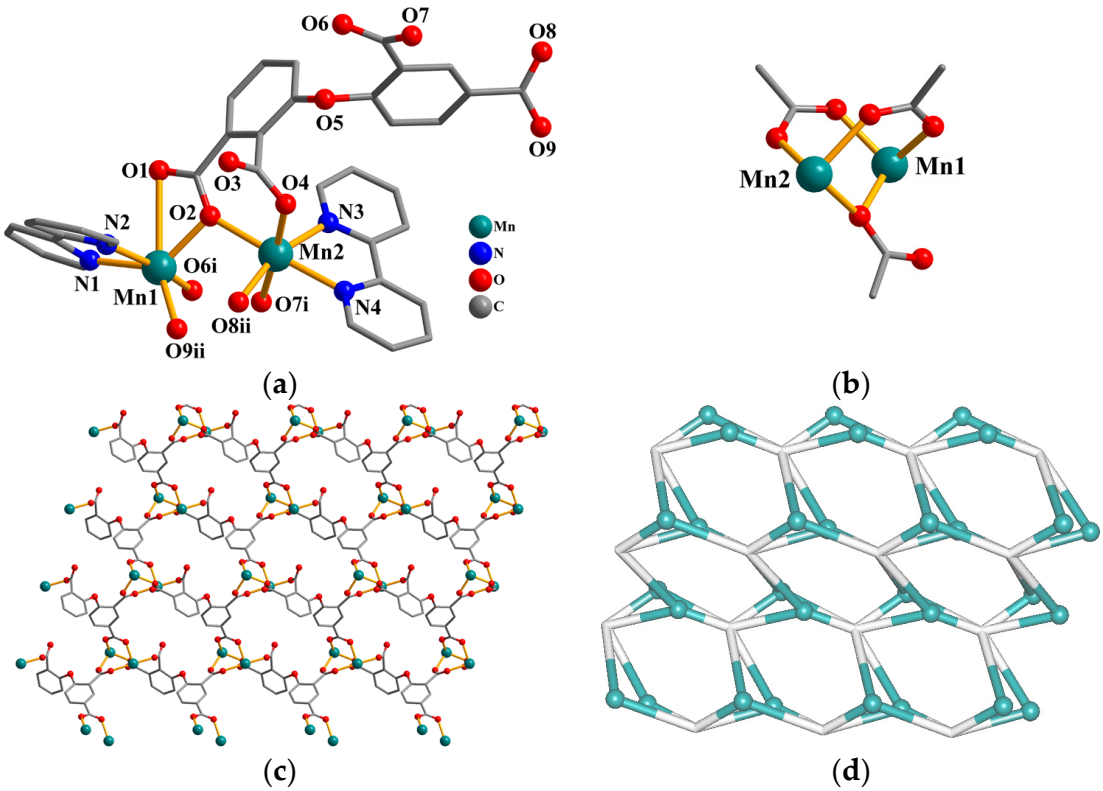

Figure 2. Structural fragments of **2**. (**a**) Coordination environment around Mn(II) atoms; H atoms are omitted for clarity. Symmetry codes: i = $x + 1, y, z$; ii = $x + 1, -y + 3/2, z + 1/2$. (**b**) Mn_2 subunit. (**c**) 2D metal-organic layer; view along the *b* axis. (**d**) Topological representation of 2D layer with a **3,6L66** topology; view along the *b* axis; Mn(II) nodes (turquoise balls), centroids of μ_6-dpa^{4-} nodes (gray).

*2.3. Structure of $[Mn_2(\mu_6\text{-dpa})(bipy)_2]_n$ (**2**)*

The structure of **2** also shows a 2D coordination polymer network (Figure 2). Per asymmetric unit, there are two manganese(II) atoms, one μ_6-dpa^{4-} block, and two bipy ligands. The Mn1 center is five-coordinated and shows a distorted $\{MnN_2O_3\}$ trigonal-bipyramidal environment. It is built from three oxygen atoms from three μ_6-dpa^{4-} linkers and a pair of bipy N donors (Figure 2a). The six-coordinate Mn2 center is bound by four oxygen atoms from three μ_6-dpa^{4-} ligands and a pair of bipy N atoms, thus creating a distorted $\{MnN_2O_4\}$ octahedral geometry. The Mn–O [2.087(3)–2.217(4) Å] and Mn–N [2.226(4)–2.277(4) Å] bonds agree with those in related compounds [19,21,22]. The tetracarboxylate dpa^{4-} moiety behaves as a μ_6-linker (Scheme 2, mode II) with the carboxylate functionalities being monodentate or μ-bridging bidentate. In μ_6-dpa^{4-}, the relevant angles are 79.83° (dihedral angle among aromatic moieties) and 116.37° (C_{ar}–O_{ether}–C_{ar}). The manganese(II) centers are held together by three carboxylate groups from three μ_6-dpa^{4-} blocks, thus generating a dimanganese(II) subunit [Mn1·Mn2 3.4679(6) Å] (Figure 2b). Such Mn_2 subunits are additionally connected by carboxylate groups of μ_6-dpa^{4-} to form a 2D metal-organic layer (Figure 2c). Regarding topology, this 2D layer is built from 3-linked Mn1/Mn2 nodes as well as the 6-linked μ_6-dpa^{4-} nodes (Figure 2d). The resulting net is thus classified as a binodal 3,6-linked layers of a **3,6L66** topological type [34]. It is described by a $(4^3.6^{12})(4^3)_2$ point symbol, wherein the $(4^3.6^{12})$ and (4^3) indices correspond to the Mn(II) and μ_6-dpa^{4-} nodes, respectively.

*2.4. Structure of $[Zn_2(\mu_4\text{-dpa})(bipy)_2(H_2O)_2]_n\cdot 2H_2O$ (**3**)*

In the structure of a 2D coordination polymer **3** (Figure 3), there are two zinc(II) atoms (Zn1, Zn2), one μ_4-dpa^{4-} block, two bipy moieties, two terminal water ligands and a couple of lattice H_2O molecules. Both Zn atoms are five-coordinated, showing

distorted $\{ZnN_2O_3\}$ square pyramidal geometries. These are constructed from two O donors from a pair of μ_4-dpa^{4-} linkers, a water ligand, and a pair of bipy nitrogen atoms. The Zn–O [1.973(3)–2.093(4) Å] and Zn–N [2.119(3)–2.181(3) Å] bond lengths are typical for compounds having an O–Zn–N environment [2,30,35,36]. The dpa^{4-} block adopts a μ_4-coordination fashion (Scheme 2, mode I). In μ_4-dpa^{4-}, the relevant angles are 72.59° (dihedral angle among two aromatic moieties) and 117.72° (C_{ar}–O_{ether}–C_{ar}). The μ_4-dpa^{4-} blocks interconnect four Zn(II) centers to furnish a 2D layer (Figure 3b). Its topological classification discloses an uninodal 3-linked layer with an **hcb** (Shubnikov hexagonal plane net/(6, 3)) topology and a (6^3) point symbol (Figure 3c) [37,38].

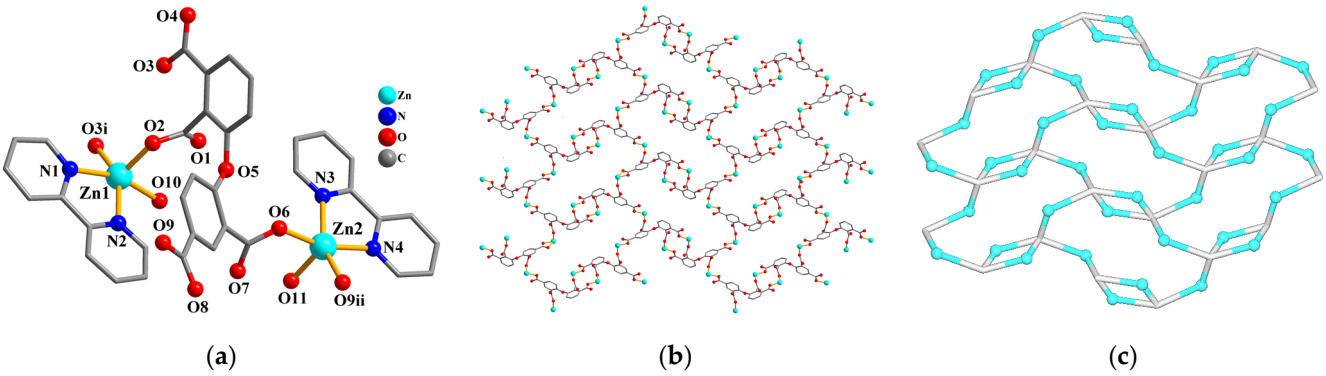

Figure 3. Structural fragments of **3**. (**a**) Coordination environment around Zn(II) atoms; H atoms are omitted for clarity. Symmetry codes: i = $-x$, $-y + 1$, $-z$; ii = $-x + 1/2$, $y - 1/2$, $-z + 1/2$. (**b**) 2D metal-organic layer; view along the *a* axis. (**c**) Topological representation of 2D layer with an **hcb** topology; view along the *a* axis; Zn(II) centers (cyan balls), centroids of μ_4-dpa^{4-} nodes (gray).

2.5. TGA & PXRD

Thermal behavior of compounds **1**–**3** was investigated by TGA on gradual heating from 30 to 800 °C under nitrogen flow (Figure S2). CP **1** reveals a loss of six lattice and one coordinated H_2O molecules in the 33–104 °C interval (calcd. 13.8%; exptl. 13.5%). After dehydration, the network of **1** maintains its stability until 220 °C. CP **2** does not encompass water as a lattice solvent or ligand and shows thermal stability up to 338 °C. For CP **3**, a mass loss in the 86–171 °C window refers to an elimination of two crystallization and two coordinated H_2O moieties (calcd. 8.4%; exptl. 8.6%); the obtained sample maintains stability until 218 °C.

To confirm a phase purity, the microcrystalline powders of **1**–**3** were analyzed by PXRD (Figure S2). The obtained experimental plots well agree with the patterns calculated from single-crystal X-ray diffraction data, what confirms a purity of the bulk solids **1**–**3** prepared via hydrothermal synthetic procedure.

2.6. Cyanosilylation of Benzaldehydes

Coordination polymers **1**−**3** were tested as catalysts in the mild, heterogeneous cyanosilylation of benzaldehyde substrates with TMSCN (trimethylsilyl cyanide) [33,35]. 4-Nitrobenzaldehyde was used as model substrate and converted into the corresponding cyanohydrin product, 2-(4-nitrophenyl)-2-[(trimethylsilyl)oxy]acetonitrile (Table 1, Scheme 3). An influence of catalyst loading, solvent type, reaction time, catalyst recycling and substrate scope was investigated.

The cyanosilylation reaction almost does not undergo when catalyst is absent or when using a carboxylic acid ligand or a metal salt precursor as potential catalysts (3−8% yields; Table 1, entries 1−3). The product yields are higher when using **1** (37%, entry 4) and **2** (27%, entry 5) as catalysts, and significantly higher in the presence of **3** (92%, entry 6). Although it is not possible to establish a clear relationship between structural features and catalytic activity of the obtained 2D compounds, we can speculate that a superior

activity exhibited by the coordination polymer **3** may eventually be related to the presence of accessible and unsaturated zinc(II) centers on a surface of catalyst particles, together with a higher Lewis acidity of the zinc sites [30,39]. Given a superior activity of zinc(II) derivative **3**, the reaction catalyzed by this CP was optimized further.

Table 1. Cyanosilylation of 4-nitrobenzaldehyde with TMSCN catalyzed by coordination polymers. [a]

Entry	Catalyst	Time, h	Catalyst Loading, mol%	Solvent	Yield [b], %
1	blank	12	-	CH_2Cl_2	3
2	H_3dpna	12	3.0	CH_2Cl_2	6
3	$ZnCl_2$	12	3.0	CH_2Cl_2	8
4	**1**	12	3.0	CH_2Cl_2	37
5	**2**	12	3.0	CH_2Cl_2	27
6	**3**	12	3.0	CH_2Cl_2	92
7	**3**	1	3.0	CH_2Cl_2	40
8	**3**	2	3.0	CH_2Cl_2	62
9	**3**	4	3.0	CH_2Cl_2	73
10	**3**	6	3.0	CH_2Cl_2	80
11	**3**	8	3.0	CH_2Cl_2	84
12	**3**	10	3.0	CH_2Cl_2	88
13	**3**	12	2.0	CH_2Cl_2	73
14	**3**	12	4.0	CH_2Cl_2	93
15	**3**	12	3.0	$CHCl_3$	82
16	**3**	12	3.0	CH_3CN	76
17	**3**	12	3.0	THF	68
18	**3**	12	3.0	CH_3OH	80

[a] Conditions: 4-nitrobenzaldehyde (0.5 mmol), TMSCN (1.0 mmol), solvent (2.5 mL), room temperature (~25 °C). [b] Yields based on ^{1}H NMR (nuclear magnetic resonance) analysis: (moles of product per mol of benzaldehyde substrate) × 100%.

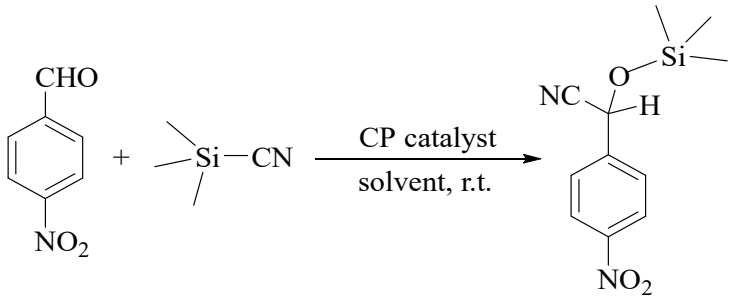

Scheme 3. Cyanosilylation of model substrate(4-nitrobenzaldehyde) into the corresponding cyanohydrin.

We found that there is an yield growth from 40 to 92% on increasing the time of reaction in the 1–12 h interval (Table 1, entries 6−12; Figure S7). The catalyst **3** loading of 2, 3, or 4 mol% has also a notable effect as attested by an yield increase from 73 to 92 and 93%, respectively (entries 6, 13, 14). Although dichloromethane (CH_2Cl_2) was used as a standard solvent to achieve the highest yield (92%), the cyanosilylation reaction also undergoes quite effectively in alternative solvents such as chloroform ($CHCl_3$, 82%), tetrahydrofuran (THF, 68%), acetonitrile (CH_3CN, 76%), and methanol (CH_3OH, 80%) (Table 1, entries 15−18).

Furthermore, in the reactions catalyzed by **3**, substrate scope was studied using different functionalized benzaldehydes (Table 2). The corresponding cyanohydrin products are obtained in yields ranging from 51 to 87%. The substrates with an electron-withdrawing group (R = NO_2, Cl) generally show a higher reactivity (Table 2, entries 2−5), which can be explained by an increased substrate electrophilicity. As expected, benzaldehyde (R = H) and substrates with an electron-donating group (R = OH, CH_3) reveal lower product yields (entries 6, 7).

Table 2. Substrate scope in cyanosilylation of various benzaldehydes with TMSCN catalyzed by **3**. [a]

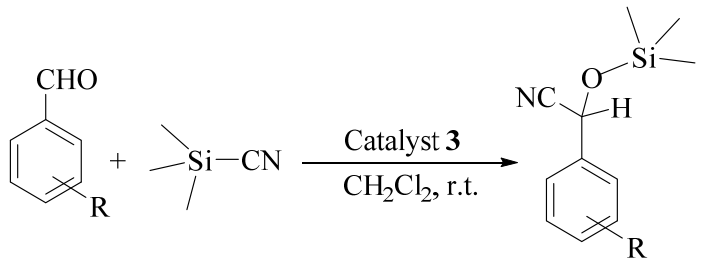

Entry	Substrate (R-C_6H_4CHO)	Yield [b], %
1	R = H	61
2	R = 2-NO_2	82
3	R = 3-NO_2	87
4	R = 4-NO_2	92
5	R = 4-Cl	62
6	R = 4-OH	56
7	R = 4-CH_3	51

[a] Conditions: functionalized benzaldehyde (0.5 mmol), TMSCN (1.0 mmol), catalyst **3** (3.0 mol.%), CH_2Cl_2 (2.5 mL), room temperature (~25 °C). [b] Yields based on ^{1}H NMR analysis: (moles of product per mol of functionalized benzaldehyde substrate) × 100%.

Given a remarkable activity of CP **3** in these cyanosilylation reactions, the stability of the catalyst and its possible recycling were studied. Thus, in the end of the cyanosilylation of 4-nitrobenzaldehyde (conditions of entry 6, Table 1), the catalyst was isolated via centrifugation, washed by CH_2Cl_2, air-dried, and reused in the next reaction runs. These tests indicate that the coordination polymer **3** behaves as a stable catalyst which maintains its activity for a minimum of 4 cyanosilylation cycles, as attested by resembling product yields in the 92−87% range (Figure S8). In addition, PXRD data of the used catalyst (Figure S9) show that its metal-organic structure remains stable.

3. Experimental

3.1. Chemicals & Equipment

All chemicals were obtained from commercial sources. In particular, 3-(2′,4′-Dicarboxy lphenoxy)phthalic acid (H_4dpa) was acquired from Jinan Henghua Sci. & Tec. Co., Ltd. (Jinan, China). Infrared (IR) spectroscopy measurements (KBr discs) were performed on a Bruker EQUINOX 55 spectrometer (Bruker Corporation, Billerica, MA, USA). Elemental analyses (C, H, N) were carried out on an Elementar Vario EL device (Elementar, Langenselbold, Germany). LINSEIS STA PT1600 thermal analyzer (Linseis Messgeräte GmbH, Selb, Germany) was used for TGA (thermogravimetric analysis) measurements under N_2 atmosphere at 10 °C/min heating rate. Excitation/emission spectroscopic data were obtained using an Edinburgh FLS920 fluorescence spectrometer (Edinburgh Instruments, Edinburgh, England). Rigaku-Dmax 2400 diffractometer (Cu-Kα radiation; λ = 1.54060 Å; Rigaku Corporation, Tokyo, Japan) was used to obtain powder X-ray diffraction (PXRD) patterns. Solution ^{1}H NMR (nuclear magnetic resonance) spectra were measured on a JNM ECS 400M spectrometer (JEOL Ltd., Tokyo, Japan).

3.2. Hydrothermal Synthesis & Analytical Data

In a general procedure, metal(II) chloride (0.2 mmol: $CuCl_2{\cdot}2H_2O$ (34.1 mg) for **1**, $MnCl_2{\cdot}4H_2O$ (39.6 mg) for **2**, or $ZnCl_2$ (27.3 mg) for **3**), H_4dpa (0.1 mmol, 34.6 mg), bipy (0.2 mmol, 31.2 mg), NaOH (0.4 mmol, 16.0 mg), and H_2O (10 mL) were added into a Teflon-lined stainless steel vessel (volume: 25 mL) and stirred for 15 min at ambient temperature. Then, the vessel was closed and kept in an oven at 160 °C. After 3 days at this temperature, the vessel was gradually (10 °C/h) cooled down to ambient temperature. The reaction

mixture was then transferred to a glass flask and the crystals of products were decanted or filtered off, followed by washing with H_2O and drying in air to produce compounds **1**−**3**.

*[Cu$_2$(μ$_4$-dpa)(bipy)$_2$(H$_2$O)]$_n$·6nH$_2$O (**1**).* Blue block-shaped crystals, yield: 55% based on H_4dpa. Calcd for $C_{36}H_{36}Cu_2N_4O_{16}$: C 47.63, H 4.00, N 6.17%. Found: C 47.86, H 3.98, N 6.21%. IR (KBr, cm^{-1}): 3748 w, 3082 w, 1599 s, 1568 s, 1497 w, 1475 w, 1448 m, 1368 s, 1288 w, 1240 m, 1164 w, 1137 w, 1084 w, 1062 w, 1032 w, 974 w, 921w, 854 w, 823 w, 770 m, 735 w, 663 w.

*[Mn$_2$(μ$_6$-dpa)(bipy)$_2$]$_n$ (**2**).* Yellow block-shaped crystals, yield: 52% based on H_4dpa. Calcd for $C_{36}H_{22}Mn_2N_4O_9$: C 56.56, H 2.90, N 7.33%. Found: C 56.37, H 2.89, N 7.38%. IR (KBr, cm^{-1}): 1639 s, 1598 s, 1569 m, 1470 w, 1438 w, 1376 s, 1240 m, 1182 w, 1157 w,1128 w, 1087 w, 1063 w, 1013 w, 968 w, 923 w, 848 w, 820 w, 770 m, 736 w, 696 w, 675 w, 646 w.

*[Zn$_2$(μ$_4$-dpa)(bipy)$_2$(H$_2$O)$_2$]$_n$·2nH$_2$O (**3**).* Colorless block-shaped crystals, yield: 48% based on H_4dpa. Calcd for $C_{36}H_{30}Zn_2N_4O_{13}$: C 50.43, H 3.53, N 6.53%. Found: C 50.64, H 3.55, N 6.51%. IR (KBr, cm^{-1}): 3383 w, 3106 w, 1614 s, 1569 s, 1470 m, 1438 s, 1392 s, 1322 w, 1244 w, 1157 w, 1083 w, 1063 w, 1021 w, 972 w, 918 w, 877 w, 766 m, 733 w, 687 w, 650 w.

3.3. Single-Crystal X-ray Diffraction

For CPs **1**–**3**, data were collected on a Bruker APEX-II CCD diffractometer (Bruker, Karlsruhe, Germany) (graphite-monochromated CuK_α radiation, λ = 1.54178 Å). SADABS was used for semi-empirical absorption corrections. Crystal structures were determined by direct methods, followed by the refinement (full-matrix least-squares on F^2) with SHELXS-97 and SHELXL-97 [40]. With an exception of hydrogen atoms, all other atoms were subjected to an anisotropic refinement (full-matrix least-squares on F^2). Except hydrogen atoms in water, all H atoms were placed in calculated positions (fixed isotropic thermal parameters); these were taken into account at the final stage of full-matrix least-squares refinement in structure factor calculations. Water hydrogen atoms were found by difference maps and constrained to the respective oxygen centers. In **1**, some molecules of solvent are heavily disordered and thus were detached by applying SQUEEZE in PLATON [41]. Elemental and thermogravimetric analyses confirmed the number of crystallization H_2O molecules. For **1**–**3**, final crystal data are summarized in Table 3. Representative bond distances and angles (Table S1) as well as hydrogen bond parameters (Table S2) are listed in Supplementary Materials. CCDC-2043757–2043759 contain crystallographic data for **1**–**3**.

For topological analysis of 2D layers in **1**–**3**, an underlying net concept was followed [42]. Such simplified networks were constructed by reducing bridging ligands to their centroids and removing terminal ligands, preserving a ligand–metal center connectivity.

3.4. Catalytic Cyanosilylation

Typical reaction mixtures were prepared as follows: in a small vessel, solid catalyst (typically 3 mol%) was suspended in dichloromethane (2.5 mL) and then an aldehyde substrate (0.50 mmol) and a cyanosilylation agent trimethylsilyl cyanide (1.0 mmol) were added. The reaction was kept under stirring at room temperature (~25 °C) for the desired time. Then, the catalyst was separated by centrifugation and the filtrate was subjected to solvent evaporation under reduced pressure to form a crude solid. This solid was dissolved in $CDCl_3$ and analyzed by ^{1}H NMR spectroscopy for product quantification (for details, see Supplementary Materials, Figures S5 and S6). In the catalyst recycling experiments, the catalyst was centrifuged, washed with CH_2Cl_2, dried at room temperature, and reused in subsequent steps that were done as described above. Blank tests without any catalyst or using metal salt or H_4dpa as catalyst were also carried out for comparative purposes.

Table 3. Crystal data for CPs **1**−**3**.

Compound	1	2	3
Chemical formula	$C_{36}H_{36}Cu_2N_4O_{16}$	$C_{36}H_{22}Mn_2N_4O_9$	$C_{36}H_{30}Zn_2N_4O_{13}$
Molecular weight	907.78	764.45	857.38
Crystal system	Monoclinic	Monoclinic	Monoclinic
Space group	$P2_1/n$	$P2_1/c$	$P2_1/n$
a/Å	10.3607 (5)	10.5312 (3)	7.9352 (2)
b/Å	35.8638 (11)	21.2195 (5)	13.1264 (4)
c/Å	11.3823 (5)	15.1835 (4)	34.5048 (10)
α/(°)	90	90	90
β/(°)	116.385 (6)	107.751 (3)	94.158 (3)
γ/(°)	90	90	90
V/Å	3788.8 (3)	3231.47 (17)	3584.58 (18)
Z	4	4	4
F (000)	1624	1552	1752
Crystal size/mm	0.25 × 0.23 × 0.21	0.18 × 0.16 × 0.15	0.26 × 0.24 × 0.20
θ range for data collection	4.508–69.993	3.699–66.992	3.604–70.060
Limiting indices	$-12 \leq h \leq 12$, $-43 \leq k \leq 30$, $-13 \leq l \leq 13$	$-12 \leq h \leq 11$, $-25 \leq k \leq 25$, $-18 \leq l \leq 17$	$-8 \leq h \leq 9$, $-1 \leq 15$, $-41 \leq l \leq 40$
Reflections collected/unique (R_{int})	19,512/7079 (0.0494)	20,432/5753 (0.0993)	13,030/6658 (0.0337)
D_c/(Mg·cm^{-3})	1.402	1.571	1.589
μ/mm^{-1}	1.892	6.917	2.285
Data/restraints/parameters	7079/0/469	5753/0/460	6658/0/496
Goodness-of-fit on F^2	1.047	1.074	1.017
Final R indices [($I \geq 2\sigma(I)$)] R_1, wR_2	0.0537, 0.1444	0.0707, 0.1680	0.0515, 0.1169
R indices (all data) R_1, wR_2	0.0710, 0.1546	0.0901, 0.1800	0.0619, 0.1238
Largest diff. peak and hole/(e·Å^{-3})	1.195 and −0.648	0.859 and −1.089	0.857 and −1.096

4. Conclusions

In this study, we explored a still poorly studied tetracaboxylic acid, 3-(2′,4′-dicarboxyl phenoxy)phthalic acid (H_4dpa), as a multifunctional linker for the hydrothermal synthesis of new CPs. Hence, a simple synthetic procedure led to the formation of a series of copper(II), manganese(II), and zinc(II) coordination polymers. These compounds feature distinct types of 2D metal-organic layers driven by the μ_4-dpa^{4-} or μ_6-dpa^{4-} linkers, as well as different topologies ranging from **sql** (**1**) and **3,6L66** (**2**) to **hcb** (**3**).

Catalytic activity of **1**−**3** was also explored in the mild cyanosilylation of benzaldehyde substrates with TMSCN, showing that the zinc(II) CP **3** functions as an effective and reusable heterogeneous catalyst to give cyanohydrin products in up to 93% yields. The effects of various reactions parameters as well as substrate scope were studied.

As main novelty features of this work, we can highlight (i) an application of H_4dpa as an underexplored multifunctional linker for design of new CPs, (ii) a synthesis of three structurally and topologically distinct metal-organic architectures, and (iii) notable catalytic activity of a zinc(II) derivative in the cyanosilylation reactions. Besides, the obtained results widen the applications of coordination polymers in heterogeneous catalysis [43,44]. Further research on assembling related types of CPs and exploring their potential in other catalytic transformations are currently underway.

Supplementary Materials: The following data are available online at https://www.mdpi.com/2073-4344/11/2/204/s1. Figure S1: FT-IR spectra, Figure S2: TGA curves, Figures S3 and S9: PXRD patterns, Figure S4: emission spectra, Figures S5–S8: supplementary catalysis data, Tables S1 and S2: selected structural parameters for **1**–**3**. CCDC-2043757–2043759.

Author Contributions: Conceptualization, J.G., X.Z. and A.M.K.; data curation, C.L., Y.L.; funding acquisition, Y.L., J.G. and A.M.K.; investigation, C.L., X.Z., Y.L., J.G. and M.V.K.; methodology, J.G.; visualization, J.G. and M.V.K.; writing—original draft, Y.L., J.G., X.Z., M.V.K. and A.M.K.; writing—review and editing, A.M.K. All authors have read and agreed to the published version of the manuscript.

Funding: This work has been supported by Science and Technology Planning Project of Guangzhou (201904010381), the Foundation for Science and Technology (FCT) and Portugal 2020 (projects CEECIND/03708/2017, LISBOA-01-0145-FEDER-029697, PTDC/QUI-QIN/3898/2020, and UID/QUI/00100/2013). This paper has been supported by the RUDN University Strategic Academic Leadership Program.

Conflicts of Interest: The authors declare no conflict of interest.

References

1. Kaskel, S. (Ed.) *The Chemistry of Metal-Organic Frameworks, 2 Volume Set: Synthesis, Characterization, and Applications*; John Wiley & Sons: Weinheim, Germany, 2016.
2. Batten, S.R.; Neville, S.M.; Turner, D.R. *Coordination Polymers: Design, Analysis and Application*; RSC: Cambridge, UK, 2009.
3. MacGillivray, L.R.; Lukehart, C.M. (Eds.) *Metal-Organic Framework Materials*; John Wiley & Sons: Chichester, UK, 2014.
4. Janiak, C. Engineering coordination polymers towards applications. *Dalton Trans.* **2003**, *2003*, 2781–2804. [CrossRef]
5. Kitagawa, S.; Kitaura, R.; Noro, S.-I. Functional Porous Coordination Polymers. *Angew. Chem. Int. Ed.* **2004**, *43*, 2334–2375. [CrossRef] [PubMed]
6. Tibbetts, I.; Kostakis, G.E. Recent Bio-Advances in Metal-Organic Frameworks. *Molecules* **2020**, *25*, 1291. [CrossRef] [PubMed]
7. Gómez-Avilés, A.; Muelas-Ramos, V.; Bedia, J.; Rodriguez, J.J.; Belver, C. Thermal post-treatments to enhance the water sta-bility of NH2-MIL-125(Ti). *Catalysts* **2020**, *10*, 603. [CrossRef]
8. Yu, L.; Dong, X.L.; Gong, Q.H.; Acharya, S.R.; Lin, Y.H.; Wang, H.; Han, Y.; Thonhauser, T.; Li, J. Splitting mono- and di-branched alkane isomers by a robust aluminum-based metal-organic framework material with optimal pore dimensions. *J. Am. Chem. Soc.* **2020**, *142*, 6925–6929. [CrossRef]
9. Wang, H.; Li, J. Microporous Metal–Organic Frameworks for Adsorptive Separation of C5–C6 Alkane Isomers. *Acc. Chem. Res.* **2019**, *52*, 1968–1978. [CrossRef] [PubMed]
10. Cui, Y.; Yue, Y.; Qian, G.; Chen, B. Luminescent Functional Metal–Organic Frameworks. *Chem. Rev.* **2011**, *112*, 1126–1162. [CrossRef]
11. Bedia, J.; Muelas-Ramos, V.; Peñas-Garzón, M.; Gómez-Avilés, A.; Rodriguez, J.J.; Belver, C. A Review on the Synthesis and Characterization of Metal Organic Frameworks for Photocatalytic Water Purification. *Catalysts* **2019**, *9*, 52. [CrossRef]
12. Karabach, Y.Y.; Guedes da Silva, M.F.C.; Kopylovich, M.N.; Gil-Hernández, B.; Sanchiz, J.; Kirillov, A.M.; Pombeiro, A.J.L. Self-assembled 3D heterometallic Cu^{II}/Fe^{II} coordination polymers with octahedral net skeletons: Structural features, molecular magnetism, thermal and oxidation catalytic properties. *Inorg. Chem.* **2010**, *49*, 11096–11105. [CrossRef]
13. Xiao, J.-D.; Jiang, H. Metal–Organic Frameworks for Photocatalysis and Photothermal Catalysis. *Acc. Chem. Res.* **2019**, *52*, 356–366. [CrossRef]
14. Gu, J.Z.; Wen, M.; Cai, Y.; Shi, Z.F.; Arol, A.S.; Kirillova, M.V.; Kirillov, A.M. Metal−organic architectures assembled from multifunctionalpolycarboxylates: Hydrothermal self-assembly, structures, andcatalytic activity in alkane oxidation. *Inorg. Chem.* **2019**, *58*, 2403–2412. [CrossRef] [PubMed]
15. Gu, J.Z.; Wen, M.; Cai, Y.; Shi, Z.F.; Nesterov, D.S.; Kirillova, M.V.; Kirillov, A.M. Cobalt(II) Coordination Polymers Assem-bled from UnexploredPyridine-Carboxylic Acids: Structural Diversity and CatalyticOxidation of Alcohols. *Inorg. Chem.* **2019**, *58*, 5875–5885. [CrossRef] [PubMed]
16. Zhang, Y.Y.; Huang, C.; Mi, L.W. Metal-organic frameworks as acid- and/or base-functionalized catalysts for tandem reac-tions. *Dalton Trans.* **2020**, *49*, 14723–14730. [CrossRef] [PubMed]
17. Agarwal, R.A.; Gupta, A.K.; De, D. Flexible Zn-MOF Exhibiting Selective CO_2 Adsorption and Efficient Lewis Acidic Catalytic Activity. *Cryst. Growth Des.* **2019**, *19*, 2010–2018. [CrossRef]
18. Liu, J.-J.; Lu, Y.; Lu, W. Metal-dependent photosensitivity of three isostructural 1D CPs based on the 1,1′-bis(3-carboxylatobenzyl)-4,4′-bipyridinium moiety. *Dalton Trans.* **2020**, *49*, 4044–4049. [CrossRef]
19. Gu, J.Z.; Cui, Y.H.; Liang, X.X.; Wu, J.; Lv, D.Y.; Kirillov, A.M. Srtructurally distinct metal−organic and H-bonded networks derivedfrom 5-(6-carboxypyridin-3-yl)isophthalic acid: Coordination and template effect of 4,4′-bipyridine. *Cryst. Grwoth Des.* **2016**, *16*, 4658–4670. [CrossRef]
20. Han, S.-D.; Chen, Y.-Q.; Zhao, J.-P.; Liu, S.-J.; Miao, X.-H.; Hu, T.-L.; Bu, X.-H. Solvent-induced structural diversities from discrete cup-shaped Co8 clusters to Co8 cluster-based chains accompanied by in situ ligand conversion. *Cryst. Eng. Comm.* **2014**, *16*, 753–756. [CrossRef]
21. Zou, X.Z.; Wu, J.; Gu, J.Z.; Zhao, N.; Feng, A.S.; Li, Y. Syntheses of two nickel(II) coordination compounds based on a rigid linear tricarboxylic acid. *Chin. J. Inorg. Chem.* **2019**, *35*, 1705–1711.
22. Gu, J.; Gao, Z.; Tang, Y. pH and Auxiliary Ligand Influence on the Structural Variations of 5(2′-Carboxylphenyl) Nicotate Coordination Polymers. *Cryst. Growth Des.* **2012**, *12*, 3312–3323. [CrossRef]
23. Li, Y.; Wu, J.; Gu, J.Z.; Qiu, W.D.; Feng, A.S. Temperature-dependent syntheses of two manganese(II) coordination com-pounds based on an ether-bridged tetracarboxylic acid. *Chin. J. Struct. Chem.* **2020**, *39*, 727–736.
24. Hou, Y.L.; Peng, Y.L.; Diao, Y.X.; Liu, J.; Chen, L.Z.; Li, D. Side chain induced self-assembly and selective catalytic oxidation activity of copper(I)-coper(II)-N4 complexes. *Cryst. Growth Des.* **2020**, *20*, 1237–1241. [CrossRef]
25. Gu, J.Z.; Wan, S.M.; Kirillova, M.V.; Kirillov, A.M. H-bonded and metal(II)-organic architectures assembled from an unex-plored aromatic tricarboxylic acid: Structural variety and functional properties. *Dalton Trans.* **2020**, *49*, 7197–7209. [CrossRef] [PubMed]

26. Gregory, R.J.H. Cyanohydrins in Nature and the Laboratory: Biology, Preparations, and Synthetic Applications. *Chem. Rev.* **1999**, *99*, 3649–3682. [CrossRef] [PubMed]
27. Brunel, J.M.; Holms, I.P. Chemically catalyzed asymmetric cyanohydrin syntheses. *Angew. Chem. Int. Ed.* **2004**, *43*, 2752–2778. [CrossRef]
28. Lacour, M.-A.; Rahier, N.J.; Taillefer, M. Mild and Efficient Trimethylsilylcyanation of Ketones Catalysed by PNP Chloride. *Chem. Eur. J.* **2011**, *17*, 12276–12279. [CrossRef]
29. Mowry, D.T. The preparation of nitriles. *Chem. Rev.* **1948**, *42*, 189–283. [CrossRef]
30. Karmakar, A.; Paul, A.; Rúbio, G.M.D.M.; Da Silva, M.F.C.G.; Pombeiro, A.J.L. Zinc(II) and Copper(II) Metal-Organic Frameworks Constructed from a Terphenyl-4,4′′-dicarboxylic Acid Derivative: Synthesis, Structure, and Catalytic Application in the Cyanosilylation of Aldehydes. *Eur. J. Inorg. Chem.* **2016**, *2016*, 5557–5567. [CrossRef]
31. Xi, Y.M.; Ma, Z.Z.; Wang, L.N.; Li, M.; Li, Z.J. Three-dimensional Ni(II)-MOF containing anasymmetric pyridyl-carboxylate ligand: Catalytic cyanosilylation of aldehydes and inhibits human promyelocytic leukemia cancer cells. *J. Clust. Sci.* **2019**, *30*, 1455–1464. [CrossRef]
32. Gu, J.-Z.; Liang, X.-X.; Cui, Y.-H.; Wu, J.; Shi, Z.-F.; Kirillov, A.M. Introducing 2-(2-carboxyphenoxy)terephthalic acid as a new versatile building block for design of diverse coordination polymers: Synthesis, structural features, luminescence sensing, and magnetism. *CrystEngComm* **2017**, *19*, 2570–2588. [CrossRef]
33. Kirillov, A.M.; Karabach, Y.Y.; Kirillova, M.V.; Haukka, M.; Pombeiro, A.J.L. Topologically Unique 2D Heterometallic CuII/Mg Coordination Polymer: Synthesis, Structural Features, and Catalytic Use in Alkane Hydrocarboxylation. *Cryst. Growth Des.* **2012**, *12*, 1069–1074. [CrossRef]
34. Chen, J.; Li, Y.; Gu, J.; Kirillova, M.V.; Kirillov, A.M. Introducing a flexible tetracarboxylic acid linker into functional coordination polymers: Synthesis, structural traits, and photocatalytic dye degradation. *New J. Chem.* **2020**, *44*, 16082–16091. [CrossRef]
35. Yu, Y. Auxiliary ligands induced two new Zn(II) compounds with the structural variations from 2D layer to 3D framework: Syntheses, structures and photoluminescent properties. *J. Mol. Struct.* **2017**, *1149*, 761–765. [CrossRef]
36. Wang, L.-N.; Zhang, Y.-H.; Jiang, S.; Liu, Z.-Z. Three coordination polymers based on 3-(3′,5′-dicarboxylphenoxy)phthalic acid and auxiliary N-donor ligands: Syntheses, structures, and highly selective sensing for nitro explosives and Fe3+ ions. *CrystEngComm* **2019**, *21*, 4557–4567. [CrossRef]
37. Gu, J.-Z.; Liang, X.-X.; Cai, Y.; Wu, J.; Shi, Z.-F.; Kirillov, A.M. Hydrothermal assembly, structures, topologies, luminescence, and magnetism of a novel series of coordination polymers driven by a trifunctional nicotinic acid building block. *Dalton Trans.* **2017**, *46*, 10908–10925. [CrossRef]
38. Jaros, S.W.; Da Silva, M.F.C.G.; Florek, M.; Smoleński, P.; Pombeiro, A.J.L.; Kirillov, A.M. Silver(I) 1,3,5-Triaza-7-phosphaadamantane Coordination Polymers Driven by Substituted Glutarate and Malonate Building Blocks: Self-Assembly Synthesis, Structural Features, and Antimicrobial Properties. *Inorg. Chem.* **2016**, *55*, 5886–5894. [CrossRef] [PubMed]
39. Cui, X.; Xu, M.-C.; Zhang, L.-J.; Yao, R.-X.; Zhang, X.-M. Solvent-free heterogeneous catalysis for cyanosilylation in a dynamic cobalt-MOF. *Dalton Trans.* **2015**, *44*, 12711–12716. [CrossRef]
40. Sheldrick, G.M. Crystal structure refinement with SHELXL. *Acta Cryst.* **2015**, *71*, 3–8. [CrossRef]
41. Van de Sluis, P.; Spek, A.L. Platon Program. *Acta Cryst.* **1990**, *46*, 194–201.
42. Blatov, V.A.; Shevchenko, A.P.; Proserpio, D.M. Applied Topological Analysis of Crystal Structures with the Program Package ToposPro. *Cryst. Growth Des.* **2014**, *14*, 3576–3586. [CrossRef]
43. Llabrés i Xamena, F.X.; Gascon, J. (Eds.) *Metal-Organic Frameworks as Heterogeneous Catalysts*; Royal Society of Chemistry: Cambridge, UK, 2013.
44. García, H.; Navalón, S. (Eds.) *Metal-Organic Frameworks: Applications in Separations and Catalysis*; John Wiley & Sons: Weinheim, Germany, 2018.